Journal of Theoretical and Applied Information Technology
15th April 2025. Vol.103. No.7

ISSN: 1992-8645 www.jatit.org E-ISSN: 1817-3195

OPTIMIZING DEEP LEARNING MODELS FOR ACCURATE MULTICLASS BRAIN TUMOR CLASSIFICATION IN MRI IMAGES

GOKAPAY DILIP KUMAR[1], PREM SWARUP MALLIPUDI[2], SHAIK THASEENTAJ[3], POLISETTY SWETHA[4], N RAMA RAO[5], SRI KUMARAN R P[6], MUDIYALA APARNA[7]

[1,2,4]Research Scholar, School of Computer Science & Engineering (SCOPE), VIT-AP University, Amaravati, Andhra Pradesh, India.
[3]Assistant Professor, Department of Computer Science & Engineering, KL University (KLEF), Green Fields, Vaddeswaram, Guntur District, Andhra Pradesh, India.
[5]Associate Professor, Department of Computer Science and Engineering, Koneru Lakshmaiah Education Foundation, Hyderabad, Telangana, India.
[6]UG Student, School of Computer Science & Engineering (SCOPE), VIT-AP University, Amaravati, Andhra Pradesh, India.
[7]Associate Professor, Department of Computer Science & Engineering, Tirumala Engineering College, Narasaraopeta, Guntur District, Andhra Pradesh, India.

[1]gokapay.22phd7117@vitap.ac.in, [2]prem.24phd7009@vitap.ac.in, [3]thaseentaj235@gmail.com, [4]swetha.23phd7121@vitap.ac.in, [5]ramarao.n@klh.edu.in, [6]parthiban.23mis7191@vitapstudent.ac.in, [7]mudiyalaaparna.89@gmail.com

Corresponding Author : Gokapay Dilip Kumar[1]

ABSTRACT

A brain tumour is an aberrant cell mass that has the potential to become cancerous. Magnetic resonance imaging (MRI) scans are frequently used to identify brain tumours. An MRI can provide information about the abnormal growth of brain tissue. Deep learning is used to construct models for the identification and categorization of brain tumours using MRI. This makes it easier and faster to diagnose brain tumours. Brain tumours can be found more quickly and precisely by using these algorithms to analyse magnetic resonance imaging (MRI) scans, which will help patients receive better care. If brain tumours were consistently detected early and treated appropriately, the death rate might be reduced. This paper also discusses the proposed design and compares it with other models, such as DenseNet-169 and Inception-ResNet-v2. By applying the recommended models, we achieved accuracy levels of 97.52% and 96.89%. In contrast to other models, it yields the best results.
Keywords: *MRI, Deep Learning, Brain Tumor, Health Care*.

1. INTRODUCTION

The human skull is the primary component of the nervous system, but the spinal cord is also a vital component of the central nervous system (CNS), which regulates the operations of all other organs and facilitates decision-making. Brain tumours are aberrant cell masses that grow inside the hard skull of the brain [1]. Both the body's voluntary and involuntary functions are regularly regulated by the brain. The brain performs tasks like assessment, integration, organizing, and selection in its capacity as the body's command centre. There is an incredibly complex structure to the human brain. Because of the pressure a developing cancer inside the skull puts the brain at risk in both adults and children, brain tumours rank as the tenth most common cause of death. Tumours can take many different forms, but no matter how they seem, feel, or are positioned, none of them have a very high chance of survival. About 2,50,000 people suffer from brain tumours annually, and 2% of these cases are found to be malignancies [2]. The number of Americans expected to receive a brain tumour diagnosis in 2020 was estimated to be 10,300 women and 13,590 men. Australia was expected to diagnose 1,879 instances of brain tumours in 2020. The brain and central nervous system are susceptible to the development of more than a hundred distinct types of benign and

malignant tumours. There are 130 instances of brain tumours, both primary and secondary [3].

Primary Brain Tumours: These tumours originate within the brain. Brain cells may be the source of a primary brain tumour, and the cancer may become encased in these nerve cells. This kind of brain tumour is not always clearly malignant [4].
Secondary brain tumours : The most prevalent kind of brain cancer are secondary brain tumours [5]. Examples of diseases that can start in other body areas and spread to the brain include kidney, breast, and skin cancers. Secondary brain tumours always metastasis, even if benign tumours don't [6].

A thorough knowledge of brain tumors and their spread is necessary for both preventive measures and the effective performance of necessary surgical therapies. Magnetic resonance imaging (MRI) is a diagnostic technique frequently used by radiologists to assess patients who may have brain tumors. MRIs, or magnetic resonance imaging, are often used in medical imaging to identify and locate brain cancers [7]. One of the main selling points of DL-based methods is their capacity for self-learning; malignancy detection via brain MRI data analysis is becoming more and more common with these techniques. In many domains, such as medical image segmentation, deep learning offers a more accurate and superior approach to machine learning. That eliminates the error-prone nature of human prediction. In this work, a number of deep learning models for tumor detection are examined, and CNN is used to distinguish benign from malignant brain tissue [8].

2. LITERATURE SURVEY

Deep learning technique utilizing an MRI dataset for tumor detection [9]. In addition to the deep educational model, we also employed the models VGG16, MobileNet, ResNet-50, and Inception V3 [10]. Ten thousand high-resolution MRI scans were examined in order to assess their models. Every kind of sickness, including brain tumors, has its own collection of 5,000 photos. Their deep learning approach allowed them to get 100% training accuracy and 98% test performance.

In this study, meningiomas, gliomas, and pituitary tumors were identified with an overall accuracy of 91.3% with recalls of 88.0%, 81.0%, and 99%, respectively, using the Milletari CNN technique [11]. A 2D convolutional neural network-based deep learning architecture is used to classify brain tumors from MRI slices. This study employs a variety of methodologies, including data processing, data collection, optimization, hyper-parameter tuning, and preliminary modeling. Ten-fold cross-validation was applied to the entire dataset in order to do an additional assessment of the model's generalizability.

The approach of convolutional neural networks was introduced by [12]. In order to enhance the effectiveness of MRI-based glioma segmentation, the authors suggest a method that combines many unique convolution neural network topologies. Their method estimates the label of each pixel using both local and global brain cell information.

Meningiomas, gliomas, and pituitary tumors may be diagnosed using a variety of methods, as demonstrated by [13]. In order to extract latent characteristics from photographs and pick features, convolutional neural networks (CNNs) were employed. The authors employed a 0.01 learning rate across ten epochs of sixteen iterations each, using the architecture that was previously described. The data collection that Cheng supplied was also used in this study. Thirty percent of the data were used for system testing, while the remaining seventy percent were used for training. The model's efficacy was assessed using the tenfold cross validation technique. Comparing the recommended method to MLP, Stacking, XGBoost, SVM, and RBF, the study finds that it is the most accurate (93.68 percent).

A CNN and a traditional architecture are combined to build a deep neural network topology utilizing the state-of-the-art correlation learning technique (CLM), which was developed by Wozniak M et al., 2023. Meningiomas (708 photographs), pituitary tumors (930 pictures), and gliomas (1,426 pictures) were identified among the 3064 instances of brain cancer that were examined. A CLM model with around 96% accuracy, 95% precision, and 95% recall was developed by them.

Hashem Zehi R. Being the supreme regulator of all physiological processes, the brain is vital to life. Across both voluntary and involuntary bodily functions, the brain serves as the primary nervous system command center [14]. A fibrous, uncontrolled mass of unwanted tissue that has spread across the entire brain is what our brain tumor is. Radiologists often utilize MRIs to find and track brain cancers so they can be treated early. A brain tumor is definitely there, as our examination has conclusively shown.

In a different study, G. Hemanth used a convolution neural network to segment pictures [15]. The least amount of pre-processing is necessary in order to explicitly extract features from photographs that are composed solely of pixels. The system makes use of LinkNet, a deep network that is comparatively lightweight. LinkNet Network Blocks, which consist of encoders and decoders and allow the image to be broken down and rebuilt multiple times before being routed via a few final rounds of convolution, form the basis of a neural network designed for semantic segmentation. The effectiveness of the recommended convolution neural networks is measured using Root Mean Square Error (RMSE), recall, sensitivity, precision, F-score specificity, and PME (probability of the misclassification error) [16].

did research at Indian Pives, Kennedy Space Centre, and Pavia University. The accuracy of CNN, which was employed, was found to be 88.75%. The information utilized in came from the Cancer Imaging Archive (TCIA). It makes use of classifiers such as SVM, RF, LOG, MLP, and PCA. The methodology used was KNN. The suggested method's overall accuracy was 83%. With a CNN (Convolutional Neural Network), we achieved an 84.19 percent accuracy increase.

According to research by [17], brain tumor pictures in MRI data have been successfully identified by EfficientNet, a dense CNN-based network. The researchers' dense EfficientNet fared better, despite the evaluation of ResNet-50, MobileNet, and MobileNetV2. By using a deep EfficientNet model, they were able to increase their efficiency and F1-score to 98.78 percent and 98 percent, respectively. To identify brain tumors, the researchers employed four different MRI methods (Sajid et al., 2019). The library included 3,260 magnetic resonance (MR) pictures. Table 1 provides an overview of the literature survey related to Brain Tumour diagnostic methodologies.

Table 1. Summary of Literature Survey

Reference	Approach/Model Used	Dataset Details	Performance Metrics	Key Findings	Limitations
Almadhoun et al.	DL, VGG16, MobileNet, ResNet-50, Inception V3	10,000 MRI scans, each cancer type has a gallery of 5,000 images	Training accuracy: 100%, Test performance: 98%	Demonstrates the effectiveness of deep learning models for classification	Limited diversity in datasets, overfitting risks
Milletari	CNN	MRI slices, ten-fold cross-validation	Overall accuracy: 91.3%, Recalls: 88.0% (Meningioma), 81.0% (Glioma), 99% (Pituitary tumors)	Shows improvement in segmentation techniques	Needs vast computational resources
Derikvand, F.	Convolutional Neural Networks	15,000 MRI Images	Enhanced performance for glioma segmentation	Useful for precise glioma detection	Does not generalize to other brain tumor types
Pashaei et al.	CNN	Data set provided by Cheng, 30% for testing, 70% for training	Accuracy: 93.68%	High classification accuracy	Limited interpretability of CNN models
Wozniak et al.	Correlation Learning Method (CLM)	3064 cases (Meningiomas: 708, Gliomas: 1426, Pituitary tumors: 930 images)	Accuracy: 96%, Precision: 95%, Recall: 95%	Effective method for brain tumor classification	Not tested on external datasets
G. Hemanth	Convolution Neural Network, LinkNet	MRI Images	RMSE, Recall, Sensitivity, Precision, F-score, Specificity, PME	Efficient segmentation method	Needs high-quality labeled data

Chen, Y.	CNN	Data from Cancer Imaging Archive (TCIA)	Accuracy: 88.75%	Good generalization ability	Comparatively lower accuracy than other models
Nayak et al.	EfficientNet, ResNet-50, MobileNet, MobileNetV2	3,260 MR images	Efficiency: 98.78%, F1-score: 98%	Efficient model with high performance	Needs further test ing on larger datasets

3. PROPOSED METHODOLOGY

Fig. 1 depicts the proposed research methodology. The major components of this study include an MRI image collection for brain tumours, image preprocessing, feature extraction, and classifier evaluation.

Figure 1 shows how the dataset is used to choose the input images, before moving on to the crucial pre-processing stage, where the data is collected. Because they were pulled from a database, the MR images were blurry and of poor quality [18]. The images were then normalized so that they could be processed further. Data is trained and tested to ensure the desired level of accuracy has been attained after feature extraction and preprocessing. After comparing the accuracy, the ill image is taken from the data set i.e 4 classes: No Tumor, Glioma, Meningioma, Pituitary. The performance and interpretability of machine learning models are improved by data preprocessing, which raises the reliability and quality of the data. Feature extraction is the preprocessing phase that condenses raw data into a smaller collection of more meaningful and representative qualities for analysis or modeling. In order to do this, relevant data must be found in the original dataset and selected, with redundant or superfluous data being removed. Feature extraction strategies are meant to extract the most important components of the data—correlations, patterns, or features—from the data in a more streamlined and structured way. Feature extraction reduces the dimensionality of the data by focusing on its most significant elements, highlighting relevant traits, and so streamlining additional analytical tasks while improving the efficiency of machine learning algorithms.

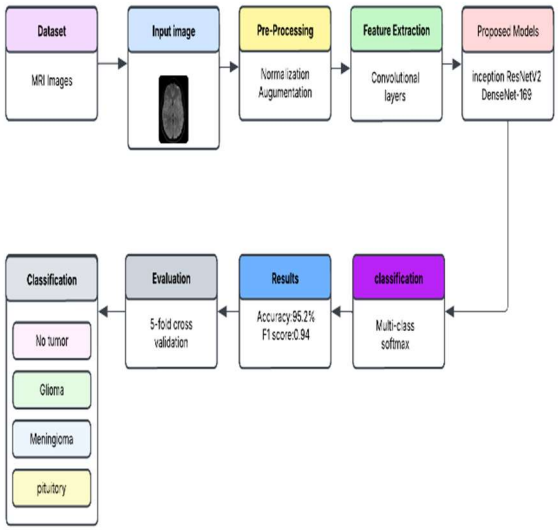

Figure 1. Flowchart of Proposed Methodology

3.1 Data Set Description

Information was collected from the Kaggle website. Brain tumour MRI scans are part of this data set. There are a total of 7023 images in this collection, and they have been labelled into four categories: Normal, Glioma, Meningioma, and Pituitary [19]. After that, we divide the functionality in two: 30% in the test dataset and 70% in the train dataset [20]. Figure 2 illustrates four different classes of MRI images used for diagnosing brain tumors.

Table 2. Classifying MRI Images into Four Categories for Training and Testing

S.No	Train /Test	Classification	No of Images	Total	%
1	Training	No Tumor	1595	5712	70
		Glioma	1321		
		Meningioma	1339		
		Pituitary	1457		
2	Testing	No Tumor	405	1311	30
		Glioma	300		
		Meningioma	306		

		Pituitary	300		
Total				7023	100

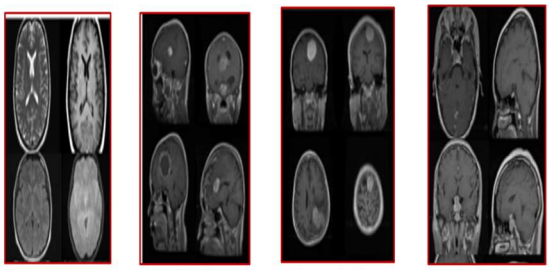

Figure 2. Pre-processing of MRI Images on Brain tumor

3.2 inception resnetv2

The Inception ResNetv2 model has a second iteration, known as Inception Resnetv2. When compared to the original inception module, it was presented with a residual connection, which substantially accelerates training while maintaining the effectiveness of attaining the ideal sparse structure with accessible, dense components in the inception module. The following figure-3 illustrates the Inception ResNetv2 layered architecture. The Inception-ResNetv2 convolutional neural network (CNN) architecture is incredibly complicated, combining two ground-breaking models—Google's Inception and Microsoft's ResNet. This model leverages both architectures benefits to achieve exceptional performance in image recognition tasks. Inception-ResNetv2 presents a main improvement by including residual connections into the Inception modules [21]. Remaining connections let information to travel directly across layers, helping Inception-ResNetv2 effectively avoid the vanishing gradient issue that occurs while training extremely deep networks. The network can retain computational efficiency and catch intricate patterns at different sizes thanks to these modules. Inception-ResNetv2 has demonstrated state-of-the-art performance on benchmark image recognition datasets, proving its ability to provide better accuracy and more generalization than previous models. These successes demonstrate how important it is to include state-of-the-art architectural elements to improve the performance of deep learning models in computer vision applications. The design integrates the Inception module's multi-scale feature extraction capabilities with the residual connections created by ResNet. This combination allows for both network-wide dissemination and effective feature representation. Inception-ResNetv2 has typical convolutional layers together with residual connections in each stacked module. These are followed by modules for average pooling and a classification layer. With its deep structure and clever architecture, Inception-ResNetv2 achieves state-of-the-art performance, outperforming its predecessors in several image recognition tasks. The reason for this architecture's success might be because it can extract intricate details from input images while resolving issues like fading gradients.

Journal of Theoretical and Applied Information Technology
15th April 2025. Vol.103. No.7

ISSN: 1992-8645 www.jatit.org E-ISSN: 1817-3195

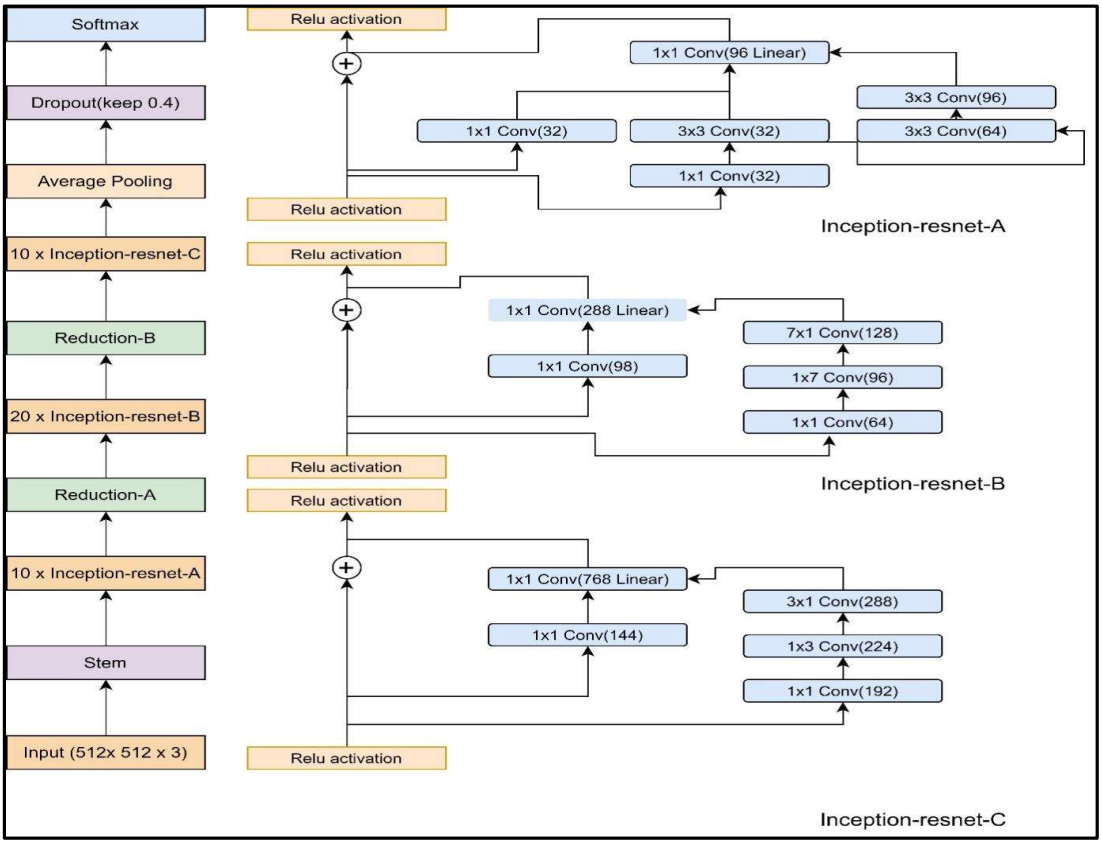

Figure 3. Basic Architecture Of Proposed Inception Resnetv2 Model

Three distinct kinds of inception modules—Inception-ResNet-A, Inception-ResNet-B, and Inception-ResNet-C—are included in the Inception-ResNetV2 model. These modules manage both the generation of the discriminatory features and the reduction of the parameters of the tiny Convolution layers (e.g., 1x7, 7x1). A distinct set of pooling and convolution layers is present in every module. Furthermore, to achieve its image-scaling magic, Inception-ResNetV2 uses not one, but two different reduction modules. The training input size for the Inception-ResNetV2 model is 512x512. below contains the Inception ResNetV2 specifications. We just require 4 classes out of the 1200 that the Inception-ResNetV2 network generated: 1. Absence of tumour 2. Glioma 3. Meningitis 4. Pituitary. our altered version Convolution layers are present in Inception-ResNetV2, 10, and 20 iterations of Inception-ResNet-A, B, and C, respectively. After that, a Softmax layer is used to counter a 3x3 max pooling layer. After the Max pooling, we employ a dropout ratio of 0.4 to mitigate overfitting. From Conv1 to FC7, the seven layers of the proposed model undergo ReLU. Mean while, the final fc layer contains four outputs that map to the four classes in the dataset.

During training, 64 images are supplied to the model at a time. Training times may be cut in half and the full model may be kept in memory when using the batch training technique. The network will be unable to determine the best global convergence state, represented in table 3, which is the function of the dropout layer has a 0.002 learning rate. Still, it will help keep the trained model more diverse and minimize overfitting. The model's dropout ratio is set at 0.4 to avoid overfitting. More trials are needed to keep the DL model from overfitting and underfitting.

When a model absorbs too much information from the training set, overfitting happens. A work around for this problem is to employ an early stopping technique, which tells us when the model stops getting better on the training dataset and starts getting better on the test dataset. Bringing together the finest features of the ResNet and Inception architectures, Inception-ResNetv2 aims to create a deep network that can capture multi-scale information while being easier to train and more computationally efficient than previous models. It has been widely used in several computer vision

applications, such as semantic segmentation, object recognition, and picture categorization.

Table 3. Inception Resnetv2 Model Layout

Type / Layer	Patch size / Stride	Input size
Conv	3×3	512×512×3
Conv	3 × 3 conv + max pool	256×256×32
Filter contact	3 × 3 pool + 3 × 3 conv	254×254×32
Filter contact	1 × 1 conv, 3 × 3 conv + 1 × 1 conv, 7 × 1 conv, 1 × 7 conv, 3 × 3 conv	254×254×64
Filter contact	3 × 3 conv + max pool	125×125×128
Inception-ResNet-A × 10	_	62×62×256
Reduction-A	_	62×62×256
Inception-ResNet-B × 20	_	31×31×768
Reduction-B	_	15×15×768
Inception-ResNet-C × 10	_	7×7×1534
Max pooling	7 × 7	7×7×1534
Dropout	Keep = 0.4	1×1×1534
Fc	1534	1534
Fc	1200	1200
Softmax	Classifier (4 classes)	600

3.3 Densenet-169

Densenet-169 is a convolutional neural network, A DenseNet architecture connects every layer to every layer below it. DenseNet-169 and the other DenseNet designs are a series of very reliable DL architectures due to their ability to address the vanishing gradient problem, their use of a robust feature propagation method, their relatively few trainable parameters, and their emphasis on feature reuse. The following figure-5 illustrates the DenseNet-169's layered architecture.

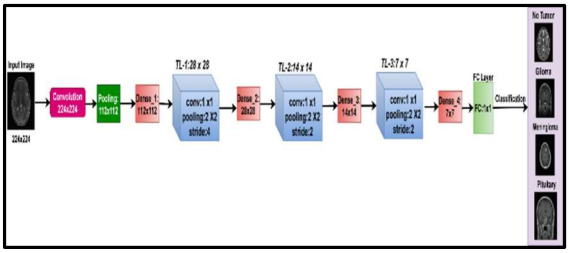

Figure 4. Basic Architecture Of Proposed Densenet-169 Model

A pooling layer and a convolutional layer comprise DenseNet-169's first layer. There are three smaller intermediate segments and four larger portions. The classification layer, the last layer of the network with a softmax activation function, connects each cluster of dense nodes to the others through transition layers. While the maxpool layers reduce the dimensionality of their inputs, the convolutional layers remove information from the image. The single array output of the flatten layer then provides fully linked layers, each of which functions as an independent artificial neural network. The layered architecture is explained in depth in table 4. One of the design's most notable features is the complex connections between the layers. In a traditional CNN, each layer is only connected to the layer that comes after it. However, with DenseNet, every layer is feed-forward linked to every other layer. Feature reuse is facilitated by this profound interconnection, as each layer takes as input the feature mappings from all preceding levels. DenseNet-169 designates its 169 layers specifically. It consists of four substantial blocks separated by a transition layer. A dense block consists of many rectified linear units (ReLU) activation functions, each of which is followed by batch normalization.

Table 4. Densenet-169 Model

Layer	Kernel Size	Parameters	Output Size
Convolution	Conv = 7 × 7	Stride = 2, Relu	224×224
Convolution	MaxPool = 2 × 2	Stride = 2, Relu	112 × 112
Pooling	MaxPool = 2 × 2	Stride = 4	56 × 56
Dense 1	Conv = 1 × 1 × 6 Conv = 3 × 3 × 6	Dropout = 0.4	56 × 56
Transition 1	Conv = 1 × 1 MaxPool = 2 × 2	Stride = 2	56 × 56 28 × 28
Dense 2	Conv = 1 × 1 × 12 Conv = 3 × 3 × 12	Dropout = 0.4	28 × 28
Transition 2	Conv = 1 × 1 MaxPool = 2 × 2	Stride = 2	28 × 28 14 × 14
Dense 3	Conv = 1 × 1 × 32 Conv = 3 × 3 × 32	Dropout = 0.4	14 × 14
Transition 2	Conv = 1 × 1 MaxPool = 2 × 2	Stride = 2	14 × 14 7 × 7
Dense 4	Conv = 1 × 1 × 32 Conv = 3 × 3 × 32	Dropout = 0.4	7 × 7
Classification	MaxPool = 1 × 1 1200D (fully connected SoftMax)		1 × 1

Convolution Layer:
A convolutional layer filters an input to activate it. After numerous applications of the filter to an input, a feature map is generated that illustrates the strength of the recognised features at various positions in the input. After creating a feature map with filters, you can activate it with a function like ReLU. A convolutional layer often conducts a dot product operation between its filter and the data it processes, which is usually much smaller than the filter.The output of an n×n square neuron component, a convolutional layer, and a m×m filter is (n-m+1) × (n-m+1). Equation (1) shows how the contributions from the cells in the topmost layer are combined to determine the nonlinear input to the unit.

$$z_{kl}^{s} = \sum_{c=0}^{m-1} \sum_{d=0}^{m-1} \mu_{c,d} y^{s-1}(K+c)(l+d) \quad (1)$$

Equation (2) illustrates how the convolutional layer implements the determined non-linearity.

$$y_{kl}^{s} = \lambda(z_{kl}^{s}) \quad (2)$$

Max-pooling Layer:
A convolutional neural network's (CNN) maxpool layer's primary objective is to minimize the dimensionality of the feature map. As a convolutional layer filters the feature map, the maxpool layer similarly gathers and summarizes relevant features. Assume that the entire numbers nh, nw, and nc. These display a feature map's proportions. The features map's dimensions are obtained by solving equation (3) after maximum pooling (maxp) over the size f and stride s filter.

$$max_p = \frac{n_h - f + 1}{s} \text{x} \frac{n_w - f + 1}{s} \text{x} n_c \quad (3)$$

Dense Layer:
Neural networks are composed of layers that are directly linked to each other by every neuron in the dense layer above it. Information travels from each thick layer neuron to its corresponding neuron, a process known as matrix-vector multiplication.

Transition Layer:
Use of simplier models is facilitated by a CNN's transition layer. The input is divided in half for the height and half for the width using a stride 2 filter and a 1x1 convolutional layer, which are common components of transition layers.

Softmax Activation Function:
Softmax activation function is one of the most often used non-linear activation functions for classification issues in deep learning networks. In general, equation (4) defines a non-linear activation function. Hence, weight and bias over an input vector Y are indicated by the letters W and B, respectively.

$$Z = f(W\ X\ Y + B) \quad (4)$$

A convolutional neural network's output layer's softmax activation function forecasts the likelihood

of each output class. A softmax is an output layer neuron that generates a single value. Each of these output layer neurons provides the probability (or likelihood) that a certain node will be the output. The data may be categorized into four groups using the softmax activation function: pituitary, meningioma, lymphoma, and no tumor.

4. RESULTS AND DISCUSSION

Using the same dataset, five models were investigated in this study. An MRI image's accuracy is measured using a brain tumour detection model. There are actually 7023 photos in the original dataset across four classes. The network is trained from scratch over the course of 30 data epochs including 280 Batches. Thirty percent is utilised for testing and seventy percent is used for training for each test. The validation set uses 15% of the training data. Tables 3 and 4 illustrate the training and testing accuracies of five models at different epochs for brain tumor analysis. Tables 2 and 5 provide a summary of the training and testing accuracy results for the models that were tested, as well as the various epoch counts that were employed. Figures (5) and (6) display graphical representations of the testing and training accuracies of each of the five models, respectively. Iterations of 10, 20, and 30 were used to train the models. After training Densenet-169 with the Inception Resnet-v2 model, we got the following results. With 96.28% training accuracy, 97.13% testing accuracy, and 97.52% overall accuracy, Inception Resnetv2 is a highly accurate model. Comparably, the Densenet169 model achieves a total accuracy of 96.89%, with training and testing accuracies of 95.12% and 96.32%, respectively. We compare the performance of multi-class classification with several widely used deep learning architectures. Out of the five models examined, the two Inception Resnetv2 and Densenet169 models in our study have the highest accuracy. Our suggested work models, Inception Resnetv2 and Densenet169, show better accuracy (97.52% and 96.89%, respectively), when compared to the current models in Table 5. The comparison results are visually represented in Figure 7. Our study dramatically improves brain tumor classification by using DenseNet169 and Inception ResNetv2, which achieve 96.89% and 97.52% accuracy, respectively, exceeding existing CNN-based models. Unlike previous research, which has focused on binary classification or small datasets, our study addresses multiclass tumor detection using a large and heterogeneous MRI dataset. Furthermore, by adding image enhancing techniques and optimization procedures, we improve model generality and resilience. These developments improve our strategy for early diagnosis and clinical applications, filling gaps in existing research and providing a dependable solution for real-world implementation.

Table 5. Training Accuracy Of Five Models On Different Epochs

S.No	Model	Epochs		
		10	20	30
1	Mobilenetv2	82.14	85.23	87.48
2	VGG16	85.34	87.28	90.03
3	Resnet50	88.43	90.34	91.27
4	Densenet169	92.31	93.46	95.12
5	Inception Resnetv2(Proposed Model)	93.16	94.65	96.28

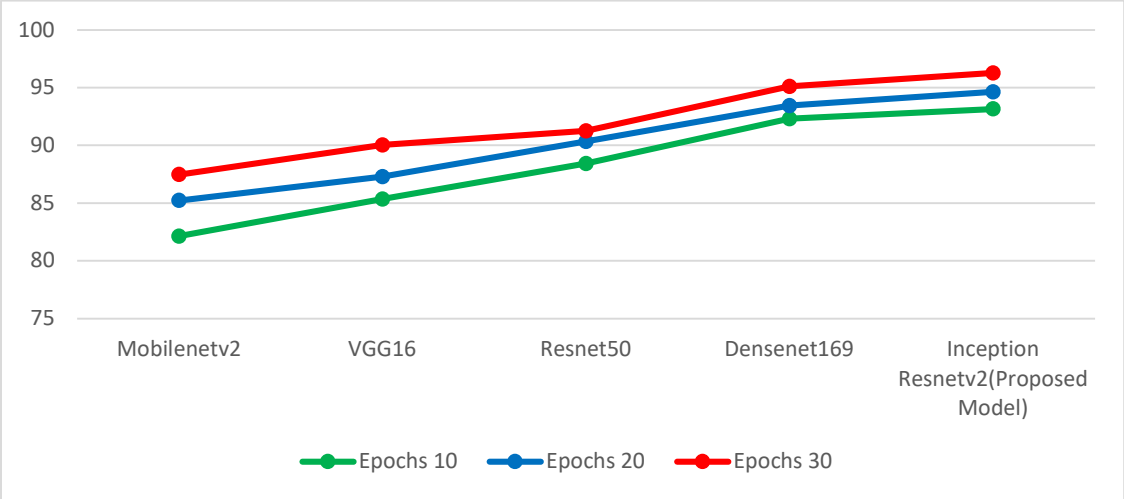

Figure 5. Graphical Representation Of Training Accuracy For Five Models On Different Epochs

Table 6. Testing Accuracy Of Five Models On Different Epochs

S.No	Model	Epochs		
		10	20	30
1	Mobilenetv2	85.65	87.92	89.23
2	VGG16	90.08	91.86	93.42
3	Resnet50	90.34	93.47	94.82
4	Densenet169	93.89	95.74	96.89
5	Inception Resnetv2(Proposed Model)	96.37	96.91	97.52

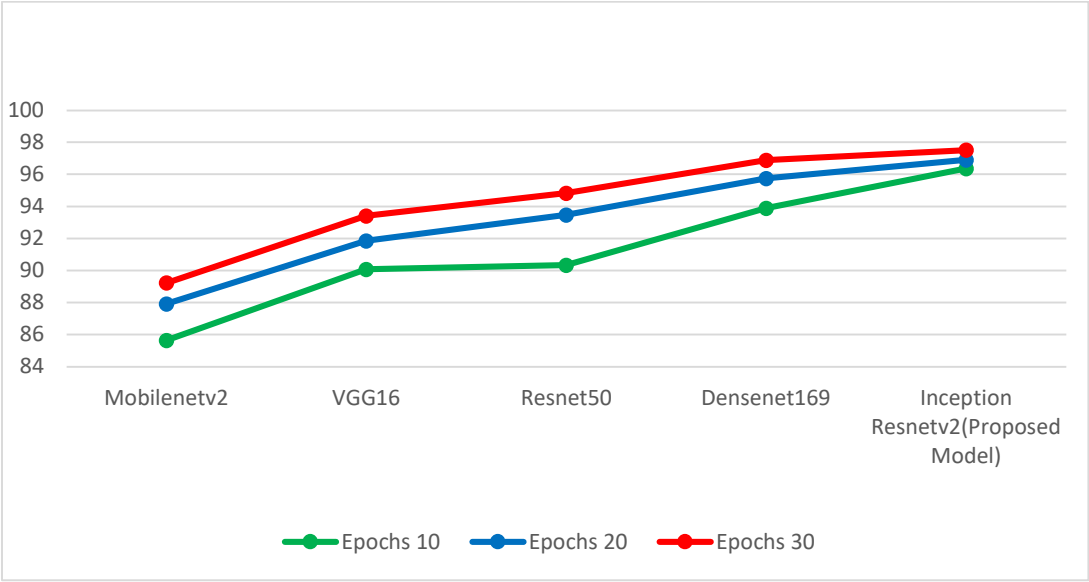

Figure 6. Graphical Representation Of Testing Accuracy For Five Models On Different Epochs

Table 7. Comparative Results Of Brain Tumor Mri Multi-Class Classification

S.No	No.of Epochs	Models	Training Accuracy	Validation Accuracy	Testing Accuracy
1	30	Mobilenetv2	87.48	88.15	89.23
2	30	VGG16	90.03	91.21	93.42
3	30	Resnet50	91.27	92.06	94.82
4	30	Densenet169(Proposed Model)	95.12	96.32	96.89
5	30	Inception Resnetv2(Proposed Model)	96.28	97.13	97.52

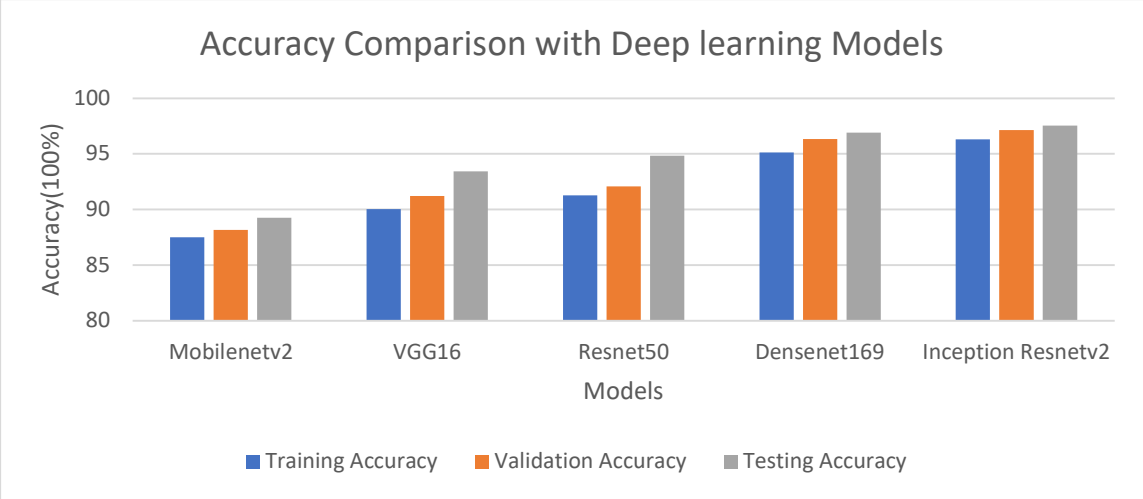

Figure 7. Graphical Representation Of Comparative Results On Brain Tumors Using MRI Images

5. CONCLUSION

A major factor in reducing mortality rates globally can be early diagnosis of brain tumors. Because of the constantly shifting size and shape of a brain tumour, accurate diagnosis of this disease remains a major challenge. Brain tumour patients clinical diagnosis and treatment decisions are profoundly influenced by the MR image classification. The tumour segmentation technique, in conjunction with MR imaging, shows promise for detection of brain tumours. Much need to be done before the precise site of the tumour can be determined and characterized. In our investigation, we searched for early indications of the disease using a range of MRI scans of brain tumours. The domains of detection and classification are also greatly impacted by deep learning models. To properly identify brain cancers at an early stage, we used a vast number of MR images and numerous deep learning models. Densenet169 and Inception Resnetv2, two deep models, were used to train and assess the network. In terms of multiclass classification, both models fared better than any other models found in the literature. We obtained 96.89% accuracy for Densenet169 and 97.52% accuracy for Inception ResNetv2. When compared to the other models, the models we suggested had the best accuracy. The Densenet169 and Inception Resnetv2 models were used to train and evaluate the network. The proposed technique enhances classification accuracy by about 2% when compared to most existing challenges. The same results can be obtained by applying picture enhancement methods and experimenting with various deep learning models. Eventually, the number of layers and filters that should be included in a particular model will be decided by optimisation algorithms. Our DL models outperform previous approaches in detecting the existence of brain tumours on the given dataset.Our study effectively achieved its goal of creating an efficient and accurate deep learning-based tumor classification classifier. However, there are several limitations, such as potential dataset overfitting and computing complexity, that may impede real-time clinical deployment. To address these issues, future research will prioritize lightweight architectures, dataset extension, and real-world clinical validation to improve the model's resilience and applicability.

Future research will focus on increasing model generalizability by including varied datasets and maximizing computing performance with lightweight architectures. Real-time deployment in healthcare contexts will be investigated using edge computing and cloud frameworks. Furthermore, explainable AI techniques will improve interpretability and assist radiologists in making decisions. Cross-validation using external datasets and multi-center trials will assure robustness and reliability

REFERENCES

[1] Abdusalomov, A. B., Mukhiddinov, M., & Whangbo, T. K. (2023). Brain Tumor Detection Based on Deep Learning Approaches and Magnetic Resonance Imaging. *Cancers*, *15*(16). https://doi.org/10.3390/cancers15164172

[2] Alsubai, S., Khan, H. U., Alqahtani, A., Sha, M., Abbas, S., & Mohammad, U. G. (2022). Ensemble deep learning for brain tumor detection. *Frontiers in Computational Neuroscience*, *16*. https://doi.org/10.3389/fncom.2022.1005617

[3] Amin, J., Sharif, M., Yasmin, M., & Fernandes, S. L. (2020). A distinctive approach in brain tumor detection and classification using MRI. *Pattern Recognition Letters*, *139*, 118–127. https://doi.org/10.1016/j.patrec.2017.10.036

[4] Aparna, M., & Rao, B. S. (2023a). A novel automated deep learning approach for Alzheimer's disease classification. *IAES International Journal of Artificial Intelligence*, *12*(1), 451–458. https://doi.org/10.11591/ijai.v12.i1.pp451-458

[5] Aparna, M., & Rao, B. S. (2023b). Xception-Fractalnet: Hybrid Deep Learning Based Multi-Class Classification of Alzheimer's Disease. *Computers, Materials and Continua*, *74*(3), 6909–6932. https://doi.org/10.32604/cmc.2023.034796

[6] Babu Vimala, B., Srinivasan, S., Mathivanan, S. K., Mahalakshmi, Jayagopal, P., & Dalu, G. T. (2023). Detection and classification of brain tumor using hybrid deep learning models. *Scientific Reports*, *13*(1), 1–17. https://doi.org/10.1038/s41598-023-50505-6

[7] Chattopadhyay, A., & Maitra, M. (2022). MRI-based brain tumour image detection using CNN based deep learning method. *Smart Agricultural Technology*, *2*(4), 100060. https://doi.org/10.1016/j.neuri.2022.100060

[8] Derikvand, F., & Khotanlou, H. (2020). Brain Tumor Segmentation in MRI Images Using a Hybrid Deep Network Based on Patch and Pixel. *Iranian Conference on Machine Vision and Image Processing, MVIP*, *2020-Febru*(Lm), 1–5. https://doi.org/10.1109/MVIP49855.2020.9116880

[9] Dhakshnamurthy, V. K., Govindan, M., Sreerangan, K., Nagarajan, M. D., & Thomas, A. (2024). *Brain Tumor Detection and Classification Using Transfer Learning Models*. 1. https://doi.org/10.3390/engproc2024062001

[10] Dipu, N. M., Shohan, S. A., & Salam, K. M. A. (2021). Deep Learning Based Brain Tumor Detection and Classification. *2021 International Conference on Intelligent Technologies, CONIT 2021*, 1–6. https://doi.org/10.1109/CONIT51480.2021.9498384

[11] Gokila Brindha, P., Kavinraj, M., Manivasakam, P., & Prasanth, P. (2021). Brain tumor detection from MRI images using deep learning techniques. *IOP Conference Series: Materials Science and Engineering*, *1055*(1), 012115. https://doi.org/10.1088/1757-899x/1055/1/012115

[12] Hashemzehi, R., Mahdavi, S. J. S., Kheirabadi, M., & Kamel, S. R. (2020). Detection of brain tumors from MRI images base on deep learning using hybrid model CNN and NADE. *Biocybernetics and Biomedical Engineering*, *40*(3), 1225–1232. https://doi.org/10.1016/j.bbe.2020.06.001

[13] Hemanth, G., Janardhan, M., & Sujihelen, L. (2019). Design and implementing brain tumor detection using machine learning approach. *Proceedings of the International Conference on Trends in Electronics and Informatics, ICOEI 2019*, *2019-April*(Icoei), 1289–1294. https://doi.org/10.1109/icoei.2019.8862553

[14] Milletari, F., Ahmadi, S. A., Kroll, C., Plate, A., Rozanski, V., Maiostre, J., … Navab, N. (2017). Hough-CNN: Deep learning for segmentation of deep brain regions in MRI and ultrasound. *Computer Vision and Image Understanding*, *164*, 92–102. https://doi.org/10.1016/j.cviu.2017.04.002

[15] Nayak, D. R., Padhy, N., Mallick, P. K., Zymbler, M., & Kumar, S. (2022). Brain Tumor Classification Using Dense Efficient-Net. *Axioms*, *11*(1). https://doi.org/10.3390/axioms11010034

[16] Pashaei, A., Sajedi, H., & Jazayeri, N. (2018). Brain tumor classification via convolutional neural network and extreme learning machines. *2018 8th International Conference on*

Computer and Knowledge Engineering, ICCKE 2018, (Iccke), 314–319. https://doi.org/10.1109/ICCKE.2018.8566571

[17] Rao, B. S., & Aparna, M. (2023). A Review on Alzheimer's Disease Through Analysis of MRI Images Using Deep Learning Techniques. *IEEE Access*, *11*(July), 71542–71556. https://doi.org/10.1109/ACCESS.2023.3294981

[18] Rehman, A., Naz, S., Razzak, M. I., Akram, F., & Imran, M. (2020). A Deep Learning-Based Framework for Automatic Brain Tumors Classification Using Transfer Learning. *Circuits, Systems, and Signal Processing*, *39*(2), 757–775. https://doi.org/10.1007/s00034-019-01246-3

[19] Sajid, S., Hussain, S., & Sarwar, A. (2019). Brain Tumor Detection and Segmentation in MR Images Using Deep Learning. *Arabian Journal for Science and Engineering*, *44*(11), 9249–9261. https://doi.org/10.1007/s13369-019-03967-8

[20] Solanki, S., Singh, U. P., Chouhan, S. S., & Jain, S. (2023). Brain Tumour Detection and Classification by using Deep Learning Classifier. *International Journal of Intelligent Systems and Applications in Engineering*, *11*(2s), 279–292.

[21] Vandana, A., Sree, V. K., Charan, S. S., & Raju, J. K. (2023). Brain Tumor Detection and Classification using Deep Learning. *14th International Conference on Advances in Computing, Control, and Telecommunication Technologies, ACT 2023*, *2023-June*, 198–203. https://doi.org/10.48175/ijarsct-3937